Electronic Supplementary Material

Synergistic effect of V and Fe in Ni/Fe/V ternary layered double hydroxides for efficient and durable oxygen evolution reaction

Lihong Chen[1], Ruxin Deng[1], Shaoshi Guo[1], Zihuan Yu[1], Huiqin Yao (✉)[2], Zhenglong Wu (✉)[3], Keren Shi[4], Huifeng Li (✉)[1], Shulan Ma (✉)[1]

1 Beijing Key Laboratory of Energy Conversion and Storage Materials, College of Chemistry, Beijing Normal University, Beijing 100875, China

2 School of Basic Medical Sciences, Ningxia Medical University, Yinchuan 750004, China

3 Analytical and Testing Center, Beijing Normal University, Beijing 100875, China

4 State Key Laboratory of High-efficiency Utilization of Coal and Green Chemical Engineering, Ningxia University, Yinchuan 750021, China

E-mails: huiqin_yao@163.com (Yao H); wuzl@bnu.edu.cn (Wu Z); lihuifeng@bnu.edu.cn (Li H); mashulan@bnu.edu.cn (Ma S)

Chemicals and materials

Iron nitrate ($Fe(NO_3)_3·9H_2O$, Macklin Chemical Reagent Co., Ltd., 98.5%), vanadium(III) chloride (VCl_3, Sigma-Aldrich Co., Ltd., 97%), urea (CH_4N_2O, Shanghai Titan Scientific Co., Ltd., 99.0%), ruthenium (IV) oxide (RuO_2, Alfa Aesar Chemical Co., Ltd., 99.9%), nafion solution (Sigma-Aldrich Co., Ltd., 5 wt%), potassium hydroxide (KOH, Xilong Scientific Co., Ltd. Co., 85.0%). All above reagents were directly utilized without further purification. Nickel foam (NF, Shenzhen Tianchenghe Technology Co., Ltd.) needs a pretreatment before being used. Firstly, untreated NF was immersed in HCl aqueous solution (1 $mol·L^{-1}$) to remove the oxidation layer. Then distilled water and absolute ethanol were successively used to ensure NF was well-cleaned. The cleaned NF was finally dried in a 60 ℃ vacuum oven.

Conventional characterization

X-ray diffraction (XRD) patterns of prepared LDH samples were obtained using a X pert pro MPD diffractometer (Cu Kα radiation, λ = 1.54056 Å), operating at 40 kV and 40 mA. The morphologies of the products were inspected using field emission scanning electronic microscope (FESEM, SU-8010, Hitachi) at an acceleration voltage of 10 kV and a high-resolution transmission electron microscope (HRTEM, Talos F200S, Thermo Fisher Scientific) at an acceleration voltage of 200 kV. X-ray photoelectron spectroscopy (XPS) spectra of the catalysts were collected using ESCALAB 250Xi spectrometer (Thermo Fisher) with Al-Kα X-ray as the radiation source.The inductively coupled plasma-atomic emission spectroscopy (ICP-AES, Jarrel-ASH, ICAP-9000) was employed to detemine the atomic ratio of Fe and V.

Method to calculate surface concentration of active sites:

Since the prepared eletrocatalysts in this work are 3d transition metal-based hydroxides showing a distinct redox peak couple before the OER onset potential, we took the redox peak method to calculate the surface concentration of active sites. The number of M(III) ions which were converted to M(II) ions is assumed to be the number of the metal sites that participate the OER catalysis. We explain the determination process of the ECSA and TOF below. Also, how the current densities be normalized by absolute ECSA is mentioned.

Determination of associated charge in the reduction region of CV:

Calculated area associated with the reduction of M(III) to M(II) for NiFeV-LDH, NiFeV-LDH, NiV-LDH and Ni foam are 0.002465, 0.002043, 0.002008, 0.0002417 VA, respectively.

Hence, their associated charges are 0.002465 VA / 0.005 Vs^{-1}, 0.002043 VA / 0.005 Vs^{-1}, 0.002008 VA /

0.005 Vs^{-1}, 0.0002417 VA / 0.005 Vs^{-1}, i.e. 0.5290, 0.4086, 0.4017, 0.04834 As (C).

Determination of the absolute ECSA by dividing elementary charge of an electron:

The absolute ECSA of NiFeV-LDH, NiFeV-LDH, NiV-LDH and Ni foam are 0.5290 C/1.602 $\times 10^{-19}$ C, 0.4086 C/1.602 $\times 10^{-19}$ C, 0.4017 C/1.602 $\times 10^{-19}$ C, 0.04834 C/1.602 $\times 10^{-19}$ C, i. e. 3.30×10^{18}, 2.55×10^{18}, 2.51×10^{18}, 3.02×10^{17}.

Normalization of current density by absolute ECSA:

To minimize the influence of the substrate (here is Ni foam), we first subtracted the absolute ECSA values of NiFeV-LDH, NiFe-LDH, NiV-LDH from Ni foam. The revised absolute ECSA values of NiFeV-LDH, NiFe-LDH, NiV-LDH are 2.998 $\times 10^{18}$, 2.248 $\times 10^{18}$, 2.208 $\times 10^{18}$, respectively. Then, we equate the absolute ECSA of NiV-LDH to 1 and those of NiFeV-LDH and NiFe-LDH to 1.358 and 1.018, respectively. Finally, the current densities are normalized by relative ECSA ($j_{\mathrm{ECSA},\ relative,}$ = j/ ECSA).

Determination of turnover frequency (TOF) from OER current density

The TOF values are calculated from the equation: TOF= $j \times N_A / F \times n \times \Gamma$.

Where j, N_A, F, n and Γ are respectively refer to current density, Avogadro number, Faraday constant, number of electrons and surface concentration of the metal sites. Note that the number of electrons of OER is four.

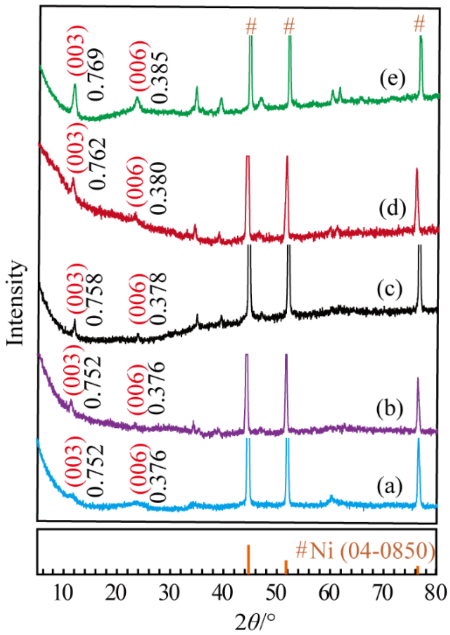

Fig. S1 XRD patterns of the as-prepared LDH samples based on different molar ratios of Fe:V: (a) 0:1, (b) 0.3:0.7, (c) 0.5:0.5, (d) 0.7:0.3, (e) 1:0.

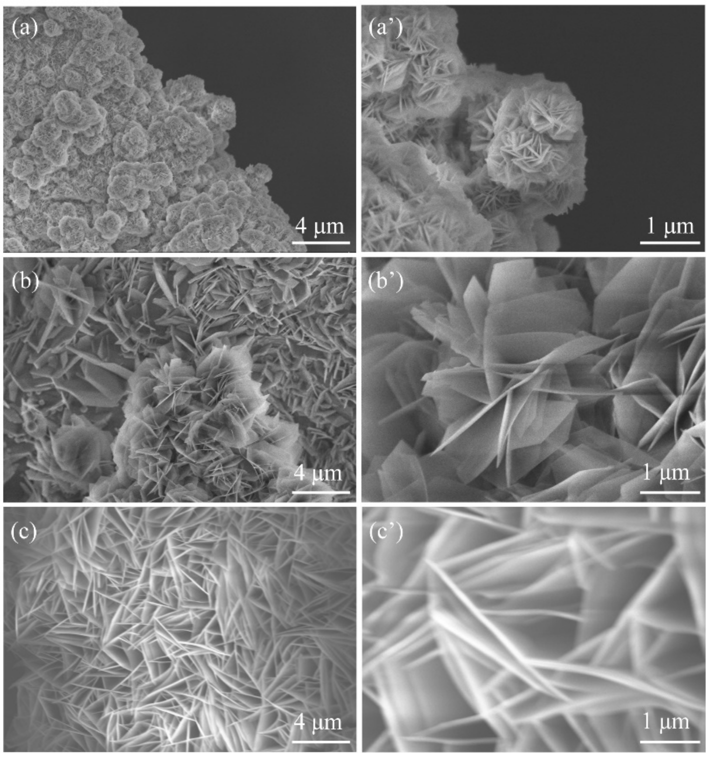

Fig. S2 SEM images of (a, a') NiV-LDH, (b, b') NiFe-LDH and (c, c') NiFeV-LDH

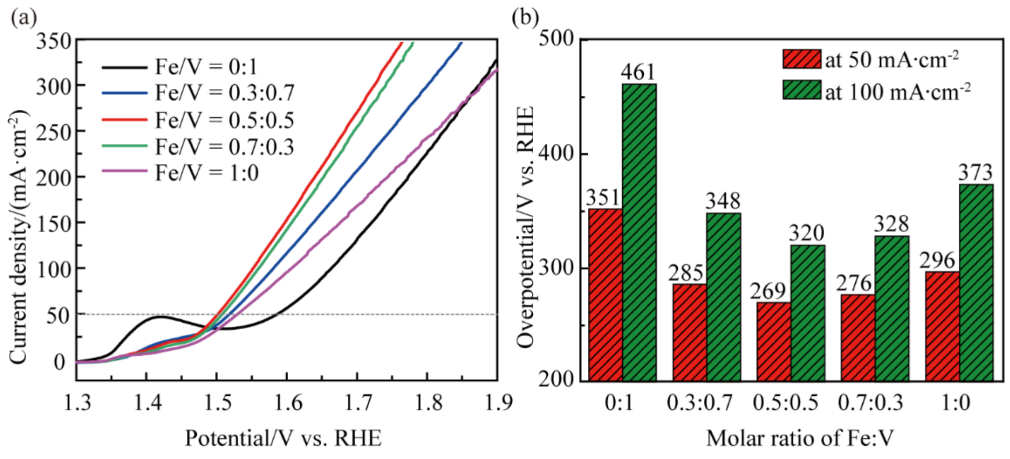

Fig. S3 (a) iR drop uncompensated OER LSV curves and (b) bar diagram of overpotentials at 50 and 100 mA·cm^{-2} of LDH samples with different Fe:V ratios.

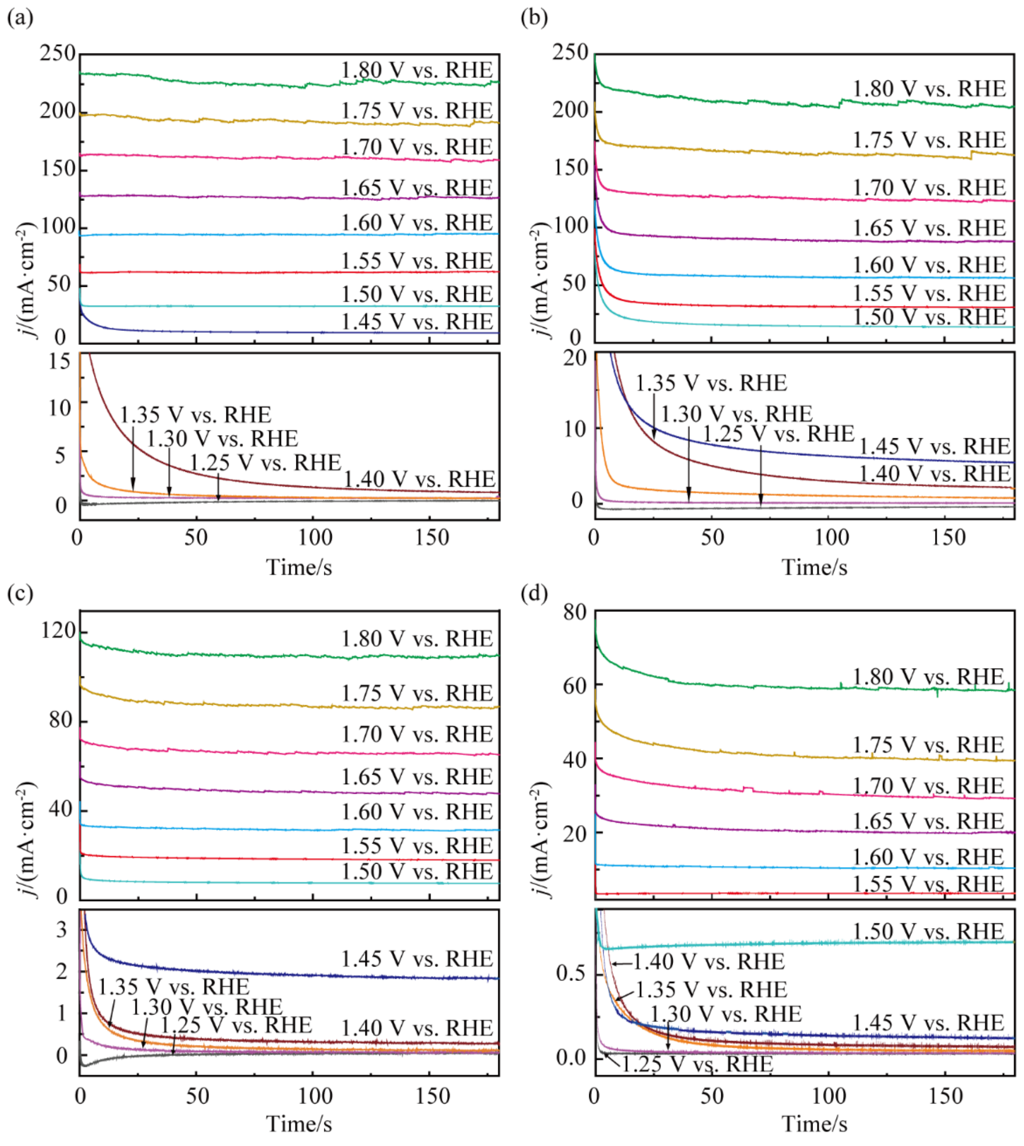

Fig. S4 CA responses of (a) NiFe-LDH, (b) NiV-LDH, (c) RuO_2 and (d) Ni foam in 1.0 M KOH for 180 s in the catalytic turnover region.

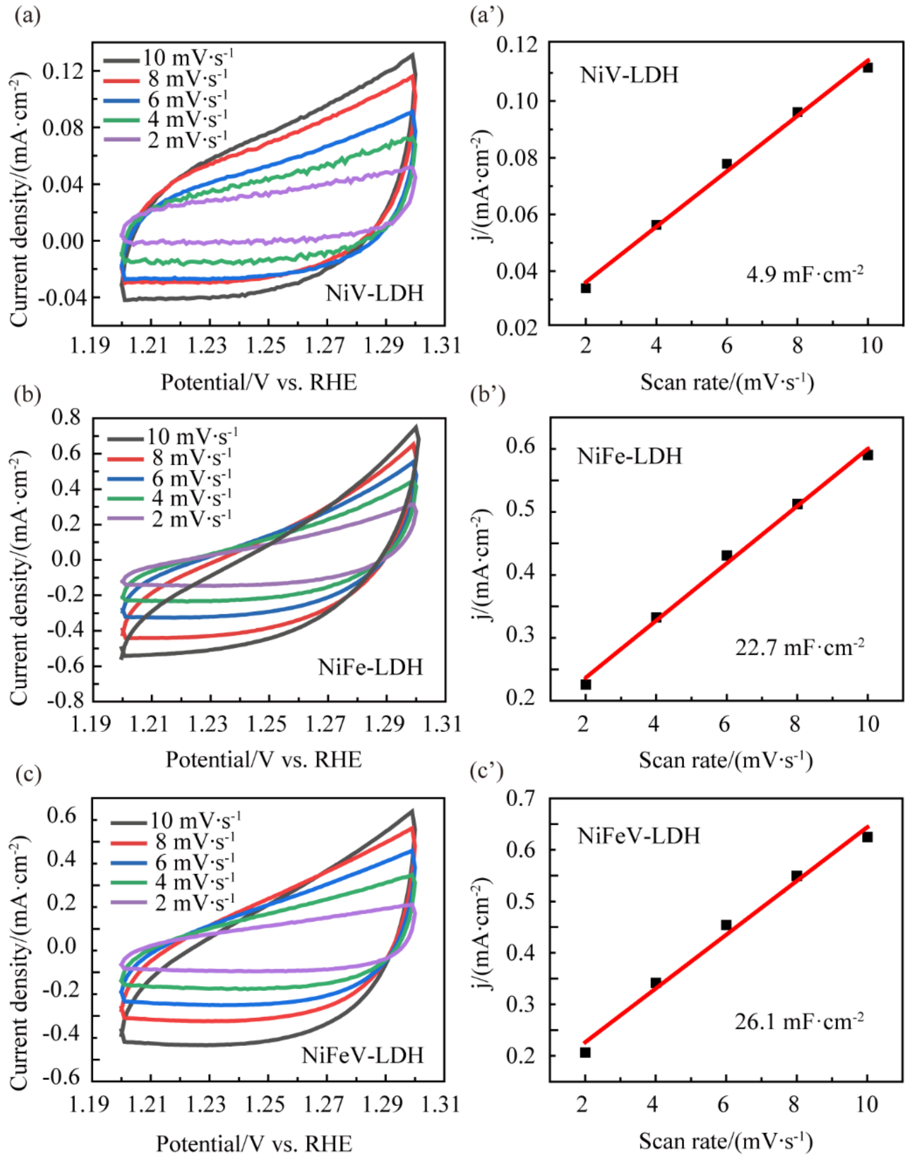

Fig. S5 CV curves of (a) NiFeV-LDH, (b) NiFe-LDH and (c) NiV-LDH with different scan rates, and corresponding Cdl calculations (a'), (b') and (c') based on the potential at 1.25 V vs. RHE.

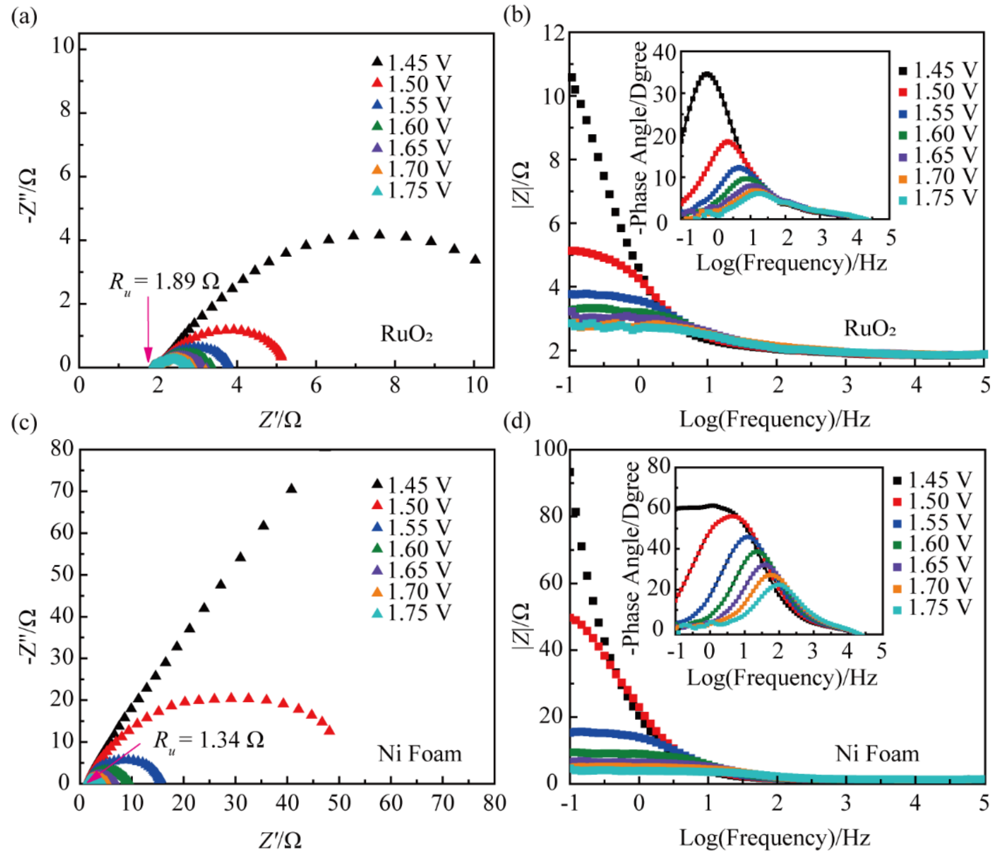

Fig. S6 Nyquist plots of (a) RuO_2 and (c) Ni foam acquired at 1.45, 1.50, 1.55, 1.60, 1.65, 1.70, 1.75 V vs. RHE and (b, d) their corresponding Bode absolute impedance plots.

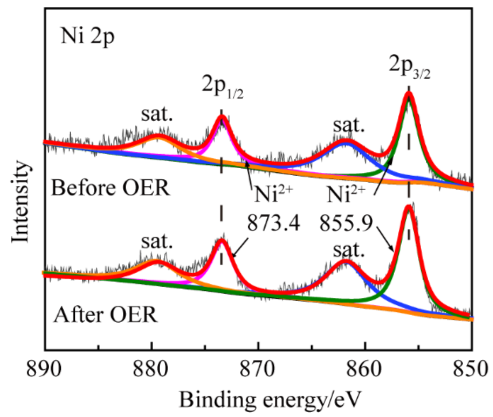

Fig. S7 XPS spectra of Ni 2p for NiFeV-LDH before and after OER durability test.

Table S1 Measured Fe:V ratio by ICP and feeding ratios for the LDH samples.

Feeding Fe:V (molar ratio)	0:1	0.3:0.7	0.5:0.5	0.7:0.3	1:0
Measured Fe:V (molar ratio)	-	0.28:0.72	0.55:0.45	0.72:0.28	-

Table S2 XPS percentages of V valence states for related electrocatalysts.

Electrocatalysts	Valance State	Area ratio (%)
	V^{3+}	13. 93
NiV-LDH	V^{4+}	41.65
	V^{5+}	44.42
	V^{3+}	24.68
NiFeV-LDH	V^{4+}	29.49
	V^{5+}	45.83
	V^{3+}	45.95
NiFeV-LDH (after OER)	V^{4+}	54.05
	V^{5+}	0.00

Table S3 Comparison of OER activity and stability of NiFeV-LDH with reported LDH-based electrocatalysts.

Catalysts	Substrates	Loading/ (mg·cm^{-2})	η_{50}/ mV	Stability time (current density)	References
NiFeV-LDH	Ni foam	1.5	269	75 h (200 mA·cm^{-2})	This work
Co^{3+}-doped NiFe-LDH	Carbon fiber paper	0.2	~335	10 h (10 mA·cm^{-2})	[1]
Co^{2+}-doped NiFe-LDH	Carbon fiber paper	0.2	~350	10 h (10 mA·cm^{-2})	[1]
Fe-doped Ni_3V_1-LDH	Glassy carbon electrode	0.28	~345	remain stable after 1000 CV cycles	[2]
Fe-Ni LDH	Ni foam	-	290	14 h (10 mA·cm^{-2})	[3]
NiFeV LDH	Ni foam	2.8	~230	18 h (187 mA·cm^{-2})	[4]
CoFeV-LDH	Ni foam	-	290	32 h (10 mA·cm^{-2})	[5]
$Ni_{0.75}Fe_{0.125}V_{0.125}$-LDH/NF	Ni foam	1.42	~270	15 h (30 mA · cm^{-2})	[6]
A-NiFeV-LDH	Ni foam	-	310	100 h (10 mA·cm^{-2})	[7]
NiFe hydroxide sheets	Ni foam	-	~260	10 h (100 mA·cm^{-2})	[8]
NiFe LDH/$NiCo_2O_4$/NF	Ni foam	4.9	290	10 h (50 mA·cm^{-2})	[9]

References

[1] Bi Y, Cai Z, Zhou D, Tian Y, Zhang Q, Zhang Q, Kuang Y, Li Y, Sun X, Duan X. Understanding the incorporating effect of Co^{2+}/Co^{3+} in NiFe-layered double hydroxide for electrocatalytic oxygen evolution reaction. Journal of Catalysis, 2018, 358: 100-107

[2] Wang Z, Liu W, Hu Y, Xu L, Guan M, Qiu J, Huang Y, Bao J, Li H. An Fe-doped NiV LDH ultrathin nanosheet as a highly efficient electrocatalyst for efficient water oxidation. Inorganic Chemistry Frontiers, 2019, 6(7): 1890-1896

[3] Zeng L, Yang L, Lu J, Jia J, Yu J, Deng Y, Shao M, Zhou W. One-step synthesis of Fe-Ni hydroxide nanosheets derived from bimetallic foam for efficient electrocatalytic oxygen evolution and overall water splitting. Chinese Chemical Letters, 2018, 29(12): 1875-1878

[4] Li P, Duan X, Kuang Y, Li Y, Zhang G, Liu W, Sun X. Tuning electronic structure of NiFe layered double hydroxides with vanadium doping toward high efficient electrocatalytic water oxidation. Advanced Energy Materials, 2018, 8(15): 1703341

[5] Hu Y, Wang Z, Liu W, Xu L, Guan M, Huang Y, Zhao Y, Bao J, Li H M. Novel cobalt-iron-vanadium layered double hydroxide nanosheet arrays for superior water oxidation performance. ACS Sustainable Chemistry & Engineering, 2019, 7(19): 16828-16834

[6] Dinh K N, Zheng P L, Dai Z F, Zhang Y, Dangol R, Zheng Y, Li B, Zong Y, Yan Q Y. Ultrathin porous NiFeV ternary layer hydroxide nanosheets as a highly efficient bifunctional electrocatalyst for overall water splitting. Small, 2018, 14(8): 1703257

[7] Zhu Y X, Liu M, Hou G Y, Tang Y P, Wu L K. The release of metal ions induced surface reconstruction of layered double hydroxide electrocatalysts. Sustainable Energy & Fuels, 2021, 5(13): 3436-3444

[8] Lu X Y, Zhao C A. Electrodeposition of hierarchically structured three-dimensional nickel-iron electrodes for efficient oxygen evolution at high current densities. Nature Communications, 2015, 6: 6616

[9] Wang Z, Zeng S, Liu W, Wang X, Li Q, Zhao Z, Geng F. Coupling molecularly ultrathin sheets of NiFe-Layered double hydroxide on $NiCo_2O_4$ nanowire arrays for highly efficient overall water-splitting activity. ACS Applied Materials & Interfaces, 2017, 9(2): 1488-1495